JOURNAL OF AGRICULTURAL AND FOOD CHEMISTRY

J. Agric. Food Chem. **2008,** *56,* 9843–9847 **9843**

Use of a Fractal-like Gold Nanostructure in Surface-Enhanced Raman Spectroscopy for Detection of Selected Food Contaminants

LILI HE,[†] NAM-JUNG KIM,[‡] HAO LI,[‡] ZHIQIANG HU,[§] AND MENGSHI LIN*,[†]

Food Science Program, Division of Food Systems and Bioengineering, Department of Mechanical and Aerospace Engineering, and Department of Civil and Environmental Engineering, University of Missouri, Columbia, Missouri 65211

The safety of imported seafood products because of the contamination of prohibited substances, including crystal violet (CV) and malachite green (MG), raised a great deal of concern in the United States. In this study, a fractal-like gold nanostructure was developed through a self-assembly process and the feasibility of using surface-enhanced Raman spectroscopy (SERS) coupled with this nanostructure for detection of CV, MG, and their mixture (1:1) was explored. SERS was capable of characterizing and differentiating CV, MG, and their mixture on fractal-like gold nanostructures quickly and accurately. The enhancement factor of the gold nanostructures could reach an impressive level of $\sim 4 \times 10^7$, and the lowest detectable concentration for the dye molecules was at ~0.2 ppb level. These results indicate that SERS coupled with fractal-like gold nanostructures holds a great potential as a rapid and ultra-sensitive method for detecting trace amounts of prohibited substances in contaminated food samples.

KEYWORDS: Gold nanostructures; SERS; crystal violet; malachite green

INTRODUCTION

Recently, there has been a growing concern about intentional contamination of foods imported into the United States. For example, imported seafood, primarily from Southeast Asia, China, Mexico, and Venezuela, have received heightened scrutiny by the Food and Drug Administration (FDA) because of the presence of harmful substances and unapproved drug residues, such as crystal violet (CV, also known as gentian violet), malachite green (MG), fluoroquinolones, and other illegal drugs (*1, 2*). CV and MG are inexpensive triphenylmethane dyes effective against fungal and parasite infections in fish (*3*). Because of their mutagenic and teratogenic effects to humans, these substances are banned for use in aquaculture (*4*). Currently, the FDA and other federal agencies routinely monitor seafood for prohibited dye residues and have set a zero-tolerance policy for all residues of CV and MG in fish. The European Commission requires that the detection methods must be able to determine the sum of MG and its main metabolite leucomalachite green (LMG) residues at the minimum performance limit of 2 parts per billion (ppb) (*5*).

Currently, liquid chromatography−mass spectrometry (LC−MS) is the principal method used by the FDA for detection and quantification of prohibited dyes in seafood samples. The limit of detection of LC−MS for dye detection could reach ~0.25 ppb (*6*). However, LC−MS is time-consuming and labor-intensive, requiring complex procedures of sample pretreatment and well-trained chemists to conduct the tests. It is therefore of significance to develop and apply a rapid, accurate, and sensitive analytical method to detect residual contaminants in food products.

Surface-enhanced Raman spectroscopy (SERS) is a promising method for rapid and sensitive detection of chemicals and biochemicals (*7, 8*). With the aid of metallic nanostructures, such as gold- or silver-based nanosubstrates, Raman signals can be enhanced by more than a million times because of spatially localized surface plasmon resonance (SPR) from the "hot spots", where huge local enhancements of the electromagnetic field are obtained (*9*). As a result, the detection limit of SERS can reach the ppb level or even the level of a single molecule (*10*). The locations of "hot spots" on the metallic structures depend upon the geometry of the nanostructures, the excitation wavelength, and polarization of the optical fields (*11*).

One of ideal nanostructures with multiple "hot spots" is the complex fractal-like nanoparticle aggregate. This intricately connected metallic structure has an extended SPR bandwidth and exhibits a strong electromagnetic coupling effect between adjacent nanoparticles. The particle junction sites are also considered to be plausible locations of "hot spots". The

* To whom correspondence should be addressed: Food Science Program, Division of Food Systems and Bioengineering, University of Missouri, Columbia, MO 65211. Telephone: (573) 884-6718. Fax: (573) 884-7964. E-mail: linme@missouri.edu.

[†] Food Science Program, Division of Food Systems and Bioengineering.

[‡] Department of Mechanical and Aerospace Engineering.

[§] Department of Civil and Environmental Engineering.

10.1021/jf801969v CCC: $40.75
Published on Web 10/02/2008

bottom−up approach based on the self-assembly phenomena has been proven to be very effective in the production of highly sensitive and cost-effective SERS nanostructures (*12*−*14*).

The objective of this study was to fabricate fractal-like gold nanostructures via a simple and cost-effective chemical synthesis method and validate the feasibility of the SERS technique coupled with fractal-like gold nanostructures to detect and characterize trace amounts of CV and MG in solution. Sensitivity of the SERS method based on self-organized gold nanostructures was evaluated, and further usage of the improved SERS-based techniques for contaminant detection was discussed.

MATERIALS AND METHODS

Preparation of Gold Nanostructures. Gold nanostructures were fabricated through a self-assembly process using gold (Au) nanoparticles as building blocks. First, gold nanoparticles with size between 30 and 50 nm were produced by a hydrothermal citrate-reduction method (*15, 16*). Sodium citrate (0.05 M) was used to reduce the gold(III) ions in 1 mM of $HAuCl_4$ aqueous solution (Sigma-Aldrich Chemicals, St. Louis, MO) by continuously stirring with a magnetic stir bar at 300 rpm at boiling temperature. The formation of gold nanoparticles was confirmed by the change of solution color from initially fainted yellow to finally wine red. The gold nanoparticle solution appeared to be stable over several months because citrate serves as a capping agent at room temperature and is capable of controlling the particle size and morphology. A small quantity (5 μL) of cetyltrimethylammonium bromide (CTAB) solution (10^{-2} M) was then introduced to the gold nanoparticle suspension in a plastic cuvette (5 mL). The color of the suspension changed immediately from wine red to blue purple, reflecting the onset of particle aggregation. As the nanoparticle aggregation proceeded, the dark-brown precipitate was gradually accumulated at the bottom of the vessel over a few hours. The precipitate was then carefully taken up by a pipet and deposited onto a clean gold-coated glass slide (Thermo Electron, Waltham, MA), and a brief annealing treatment (~300 °C, 2 h in air) was followed to provide a clean SERS-active area.

The prepared nanostructure was examined by field emission scanning electron microscopy (FESEM, FEI Quanta, OR) to verify the formation of Au nanostructures deposited on the gold-coated glass slide. A SEM scan was performed at high-vacuum mode at 10 kV of electron acceleration voltage.

Sample Preparation. CV was purchased from Fisher Scientific (Rochester, NY), and MG was purchased from MP Biomedicals (Solon, OH). Standard solutions for CV and MG were prepared and diluted in 50% ethanol solution in the range of 0.2−2000 ppb.

Raman Instrumentation. A Renishaw RM1000 Raman spectrometer system (Gloucestershire, U.K.) equipped with a Leica DMLB microscope (Wetzlar, Germany) and a 785 nm near-infrared diode laser source (maximum at 300 mW) was used in this study. Raman scattering signals were detected by a 578 × 385 pixels CCD array detector. The size of each pixel was 22 × 22 μm. Spectra of each sample were collected using a 50× objective, with a detection range from 300 to 1800 cm^{-1}. The measurement was conducted with a 10 s exposure time and ~2 mW laser power.

Data Analysis. Spectral data were analyzed by the software GRAMS 32 spectral notebase (Galactic Industries, Waltham, MA) and Delight software (D-Squared Development, Inc., LaGrande, OR). Preprocessing algorithms, such as standard normal variate and second-derivative transformation with a gap of 12 cm^{-1}, were used to normalize the spectra, separate overlapping bands, and remove baseline shifts (*17*). Principal component analysis (PCA) was then applied to analyze spectral data. The PCA procedure reduces a multidimensional data set to its most dominant features, removes random variation, and retains the principal components (PCs) that capture the variation between sample treatments (*18*).

Sensitivity of SERS Measurements. To determine the enhancement factor (EF) of this fractal-like gold nanostructure as a SERS-active substrate, ~5 μL of 2 ppb and 2000 ppm CV solutions were deposited onto the gold nanostructure, respectively. A commercial gold-coated glass slide (Thermo Electron, Madison, MI) without gold nanostructures was used as a control. EF of SERS was calculated according to the following eq 1:

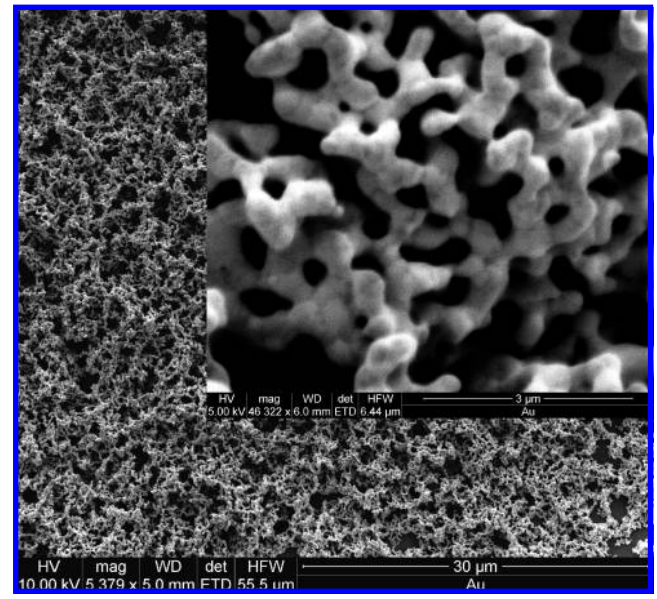

Figure 1. SEM image of a fractal-like aggregate film self-organized from gold nanoparticles. A higher magnified image of gold clusters is provided in the inset. The high-resolution SEM image reveals the formation of nanopores as a result of nanoparticle clustering through the self-assembly and coarsening effect from an annealing process.

$$\mathrm{EF} = \frac{I_{\mathrm{sers}}}{I_{\mathrm{nor}}}\frac{C_{\mathrm{nor}}}{C_{\mathrm{sers}}} \quad (1)$$

where I_{sers} and I_{nor} are the peak intensities in SERS and normal Raman spectra, respectively, and C_{sers} and C_{nor} are the analyte concentrations in the SERS and normal Raman measurements, respectively.

To evaluate the sensitivity of SERS, a series of CV concentrations (0.2, 2, 20, 200, and 2000 ppb) were deposited on the gold nanostructures and analyzed by SERS. One of the most intense peaks was examined to correlate the CV concentration with the peak intensity. The lowest concentration at which most CV characteristic peaks remained noticeable was considered as the lowest detectable concentration.

RESULTS AND DISCUSSION

Nanoscale Patterns of Gold Nanostructures. SEM images (**Figure 1**) reveal a complex but well-developed porous structure obtained from self-assembled gold nanoparticles after a brief annealing. The clustering and aggregation of nanoparticles initially took place in an aqueous solution to form a fractal-like network, and a heat-induced structural coarsening effect occurred during the annealing step, resulting in a complex porous Au structure. These porous nanostructures are expected to be useful to attract and trap analyte molecules in the close proximity of a metal surface. The pores observed under the SEM were found to be rather broad in size distribution, while the average pore size was estimated to be around 300 nm.

A previous study (*13*) reported a similar pore size of the dealloyed nanoporous gold film to exhibit the SERS effect. We believe that increasing the annealing time and/or temperature would yield larger average pore sizes as well as increase sizes of connected nanoclusters as a result of coarsening, while the heat from annealing further purges the metal surface. It is therefore important to find the best annealing condition by precisely controlling time and temperature during annealing

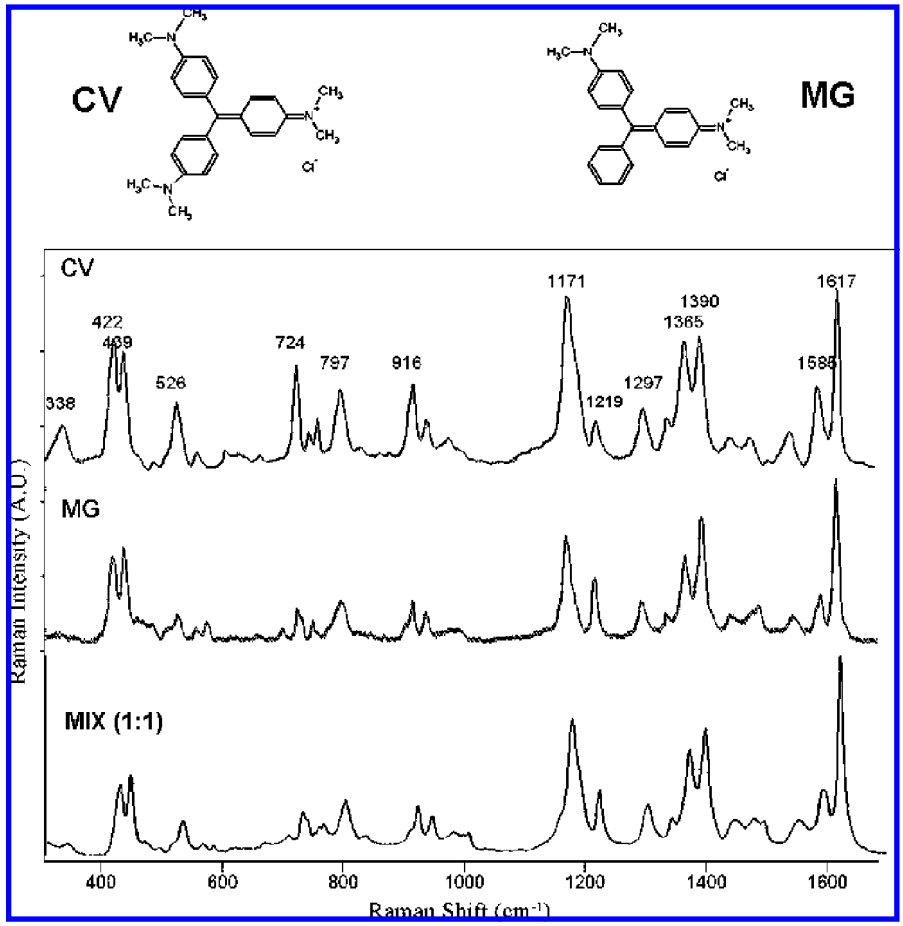

Figure 2. Average SERS spectra ($n = 8$) of 200 ppb CV, MG, and their mixure (1:1). Measurement was taken from 300 to 1800 cm^{-1} under 10 s and ~2 mW laser power.

Table 1. Band Assignments of Peaks in CV and MG Raman Spectra (*19*)

Raman shift (cm^{-1})	band assignment
~338	in-plane vibration of phenyl−C−phenyl
~422	out-of-plane vibrations of phenyl−C−phenyl
~526 and 916	ring skeletal vibration of radical orientation
~724 and 797	out-of-plane vibrations of ring C−H
~1171	in-plane vibrations of ring C−H
~1219	C−H rocking
~1365 and 1390	N−phenyl stretching
~1585 and 1617	ring C−C stretching

because the generation of the SPR is believed to be dependent upon the size of Au nanoparticles as well as the pore size of Au nanoclusters.

SERS Spectra of CV, MG, and Their Mixture (1:1). CV and MG are very similar in their molecular structures. Not surprisingly, their Raman spectra are very close to each other (**Figure 2**). Their major peak assignments were shown in **Table 1** (*19*). One noticeable difference between these two molecules in Raman spectra could be found at the peak around 338 cm^{-1} as the in-plane vibration of phenyl−C−phenyl bend, which is clearly present in CV spectra but not in those of MG (**Figure 2**). Additionally, it was found that the ratio of peak intensity of 1171 over 1219 cm^{-1}, which were assigned to be the in-plane vibrations of ring C−H and C−H rocking, respectively, was much higher in CV than that in MG. Other slight differences between relative peak intensities at several positions (e.g., 526, 724, and 916 cm^{-1}, etc.) were also found between CV and MG. These differences were likely attributed to the presence of one more CH_3−N−CH_3 in CV than in MG. When testing the spectra

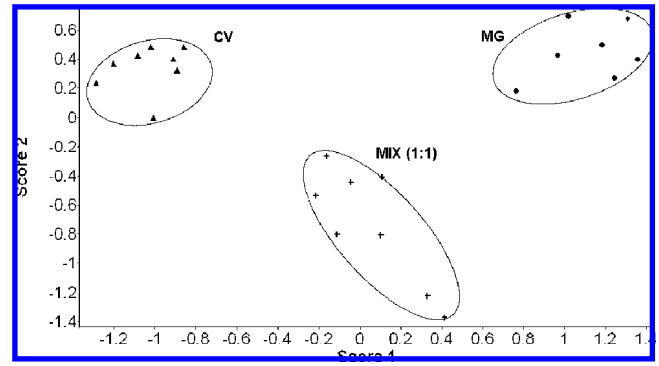

Figure 3. Two-dimensional (2D) PCA plot based on the SERS spectra of MG, CV, and the mixture of MG and CV (1:1).

of mixed samples (1:1), the changes of peak 338 cm^{-1} and the ratio of peak intensity of 1171 over 1219 cm^{-1} were clearly observed. The intensity values were found, as expected, to be the averages of those of CV and MG. The value of the ratio of peak intensity of 1171 over 1219 cm^{-1} may be used to calculate the percentages of CV and MG in the mixture.

To differentiate these two chemicals, further analysis using PCA was conducted on the basis of SERS spectral data of CV, MG, and the mixture (1:1) (**Figure 3**). PCA is a data reduction method, which captures the variation between samples based on their PCs. Segregations between CV, MG, and the mixture were clearly observed. As expected, the cluster of mixed samples was positioned in the middle between the CV and MG clusters. The first five PCs explained 80% of total data variances. These results demonstrate that chemicals with similar molecular

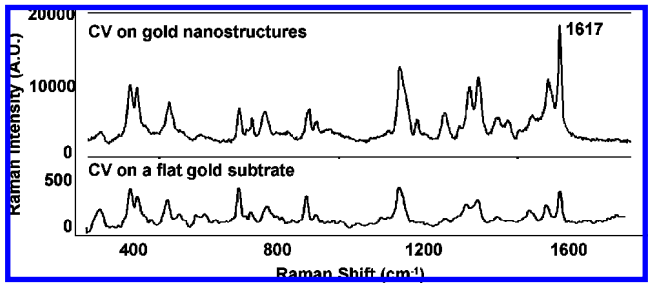

Figure 4. SERS spectrum of 2 ppb CV on gold nanostructures and a normal Raman spectrum of 2000 ppm CV on the control (a gold-coated glass slide). Both spectra were acquired under identical Raman instrumental conditions.

structures, such as CV, MG, and their mixture, can be differentiated by SERS methods in conjunction with the use of gold nanostructures.

Sensitivity of SERS Measurements. To determine the enhancement factor (EF) of this fractal-like gold nanostructure as a SERS-active substrate, 2 ppb CV solution was deposited onto a fractal-like gold nanostructure and 2000 ppm CV solution was deposited onto a control (gold-coated flat surface without nanostructures), respectively. The intensity of a peak at ~1617 cm^{-1} in the CV Raman spectrum from the gold flat surface was ~500, while from gold nanostructure, it was ~20000 (**Figure 4**). This was a substantial increase in peak resolution. On the basis of eq 1, an EF of $\sim 4 \times 10^7$ for Raman signal enhancement was calculated for the gold nanostructures applied in SERS measurements. This result clearly demonstrates that the SERS method coupled with the gold nanostructures is promising to serve as an ultra-sensitive and nondestructive analytical technique for chemical detection.

To evaluate the sensitivity and reliability of SERS and quantify different concentrations of the analyte on gold nanostructures, samples containing a series of CV concentrations (0.2, 2, 20, 200, and 2000 ppb) were deposited on the gold nanostructures and analyzed by SERS (**Figure 5**). As shown by the curve in **Figure 5**, the peak intensity at 1617 cm^{-1} increased monotonously with the increase of CV concentrations. There is a linear relationship between the log value of intensity and the log value of CV concentrations between 0.2 and 20 ppb. At the higher CV concentrations, however, a saturation of peak intensities becomes evident. Curves with similar trend were reported by others using SERS (*14, 20*). On the basis of these results, it can be inferred that SERS activities from the gold nanostructures were well-behaved at different concentration levels over 3 orders of magnitude, making it possible to quantify trace amounts of the analytes by SERS.

SERS spectra of CV exhibited distinct and characteristic Raman peaks when the concentration of CV was at the ppb level. Some Raman peaks of CV were still detectable at 0.2 ppb level, even though some interfering peaks because of background noises become evident. From the linear observation, the lowest detectable concentration on this gold nanostructure was estimated to be ~0.2 ppb, which is quite remarkable and well-satisfies the recommended detection level by the food safety regulations.

Currently, however, there are only a few tentative applications of SERS in solving food safety issues, most likely because of the lack of economic, effective, and reliable SERS-active substrates (*21, 22*). This preliminary study demonstrates that SERS coupled with fractal-like gold nanostructures has a great potential to serve as a promising analytical technique for the

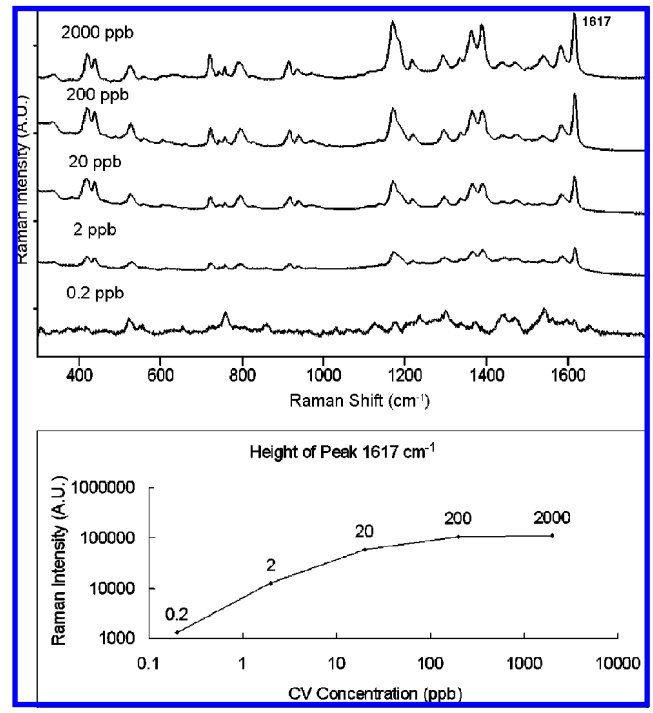

Figure 5. SERS spectra of CV at concentrations of 0.2, 2, 20, 200, and 2000 ppb on fractal-like gold nanostructures. The peak intensities increased monotonously as the concentrations of CV deposited on a nanostructure increased. Relationship between the log value of peak height at 1617 cm^{-1} and log value of the CV concentration (0.2 to 20 ppb) is also shown.

detection and characterization of trace amounts of food contaminants, such as CV and MG.

It should be mentioned that our nanoparticle-based gold nanostructures are chemically very stable and physically robust. The gold nanostructures did not show any sign of degrading SERS activities when stored at an ambient laboratory environment for days, washed with volatile cleaning solvents, such as ethanol, or agitated in an ultrasonic cleaner for several minutes. These indicate a remarkable mechanical strength of self-organized complex nanostructures. Considering the simplicity of the fabrication process and impressive ultra-high sensitivity of gold nanostructures, we expect that these self-assembled gold nanostructures will greatly promote SERS applications in detecting chemicals for food safety concern.

Several issues about the SERS-active nanosubstrates made through the "bottom−up" approach remain to be addressed. For instance, defective structural integrity over a large scale and/or poor substrate−substrate consistency may limit the use of these nanosubstrates for widespread applications (*23*). Therefore, future studies are needed to improve the reproducibility of nanosubstrates in SERS measurements and large-scale production. The multiple-interconnected gold clusters and the natural formation of pores are crucial to fabricate high-quality SERS-active nanosubstrate. Improvement of reproducibility could be achieved by fabricating nanosubstrates under optimal conditions, including controlled initial nanoparticle sizes, film thickness, and annealing temperatures. In addition, work is underway in our laboratory to apply this ultra-sensitive SERS method to detect and characterize contaminants in real food products. The major challenge for application of SERS in real foods, besides the nanosubstrates issues stated above, will be how to detect food contaminants with the presence of interferences from food components. We expect that CV and MG can be easily detected because of their multiple-ring structures and efficient adsorption

onto gold or silver surface, thus producing stronger Raman signals than other chemicals or biochemicals (*24*).

LITERATURE CITED

(1) Food and Drug Administration (FDA). Questions and answers on FDA's import alert on farm-raised seafood from China. http://www.cfsan.fda.gov/~frf/seadwpe.html (accessed June 28, 2007).

(2) Food and Drug Administration (FDA). Marketing and import information on seafoods and seafood safety. http://www.foodsafety.gov/~dms/fs-toc.html (accessed Dec 16, 2007).

(3) Alderman, D. In vitro testing of fisheries chemotherapeutants. *J. Fish Dis.* **1982**, *5*, 113–123.

(4) Culp, S.; Beland, F. Malachite green: A toxicological review. *J. Am. Coll. Toxicol.* **1996**, *15*, 219–238.

(5) Anonymous. Commission decision 2004/25/EC as regards the setting of minimum required performance limits (MRPLs) for certain residues in food of animal origin. *Off. J. Eur. Union* **2004**, *L6*, 38−39.

(6) Andersen, W.; Turnipseed, S.; Roybal, J. Quantitative and confirmatory analyses of malachite green and leucomalachite green residues in fish and shrimp. *J. Agric. Food Chem.* **2006**, *54*, 4517–4523.

(7) Bell, S.; Mackle, J.; Sirimuthu, N. Quantitative surface-enhanced Raman spectroscopy of dipicolinic acid—Towards rapid anthrax endospore detection. *Analyst* **2005**, *130*, 545–549.

(8) Zhang, X.; Shah, N.; Van Duyne, R. Sensitive and selective chem/biosensing based on surface-enhanced Raman spectroscopy (SERS). *Vib. Spectrosc.* **2006**, *42*, 2–8.

(9) Haynes, C.; McFarland, A.; Van Duyne, R. Surface-enhanced Raman spectroscopy. *Anal. Chem.* **2005**, *77*, 338–346.

(10) Kneipp, K.; Haka, A.; Kneipp, H.; Badizadegan, K.; Yoshizawa, N.; Boone, C.; Shafer-Peltier, K.; Motz, J.; Dasari, R.; Feld, M. Surface-enhanced Raman spectroscopy in single living cells using gold nanoparticles. *Appl. Spectrosc.* **2002**, *56*, 150–154.

(11) Le Ru, E.; Etchegoin, P. Sub-wavelength localization of hot-spots in SERS. *Chem. Phys. Lett.* **2004**, *396*, 393–397.

(12) Jana, N. Silver coated gold nanoparticles as new surface enhanced Raman substrate at low analyte concentration. *Analyst* **2003**, *128*, 954–956.

(13) Kucheyev, S.; Hayes, J.; Biener, J.; Huser, T.; Talley, C.; Hamza, A. Surface-enhanced Raman scattering on nanoporous Au. *Appl. Phys. Lett.* **2006**, *89*, 053102.

(14) Qiu, T.; Wu, X. L.; Shen, J. C.; Xia, Y.; Shen, P.; Chu, P. Silver fractal networks for surface-enhanced Raman scattering substrates. *Appl. Surf. Sci.* **2008**, *254*, 5399–5402.

(15) Chen, S.; Carroll, D. L. Silver nanoplates: Size control in two dimensions and formation mechanisms. *J. Phys. Chem. B* **2004**, *108*, 5500–5506.

(16) Cheng, W.; Dong, S.; Wang, E. Spontaneous fractal aggregation of gold nanoparticles and controlled generation of aggregate-based fractal networks at air/water interface. *J. Phys. Chem. B* **2005**, *109*, 19213–19218.

(17) Huang, W.; Griffiths, R.; Thompson, I.; Bailey, M.; Whiteley, A. Raman microscopic analysis of single microbial cells. *Anal. Chem.* **2004**, *76*, 4452–4458.

(18) Goodacre, R.; Timmins, E.; Burton, R.; Kaderbhai, N.; Woodward, A.; Kell, D.; Rooney, P. Rapid identification of urinary tract infection bacteria using hyperspectral whole-organism fingerprinting and artificial neural networks. *Microbiology* **1998**, *144*, 1157–1170.

(19) Liang, E.; Ye, X.; Kiefer, W. Surface-enhanced Raman spectroscopy of crystal violet in the presence of halide and halate ions with near-infrared wavelength excitation. *J. Phys. Chem. A* **1997**, *101*, 7330–7335.

(20) Tao, A.; Kim, F.; Hess, C.; Goldberger, J.; He, R.; Sun, Y.; Xia, Y.; Yang, P. Langmuir−Blodgett silver nanowire monolayers for molecular sensing using surface-enhanced Raman spectroscopy. *Nano Lett.* **2003**, *3*, 1229–1233.

(21) He, L.; Liu, Y.; Lin, M.; Awika, J.; Ledoux, D.; Li, H.; Mustapha, A. A new approach to measure melamine, cyanuric acid, and melamine cyanurate using surface enhanced Raman spectroscopy coupled with gold nanosubstrates. *Sens. Instrum. Food Qual.* **2008**, *2*, 66–71.

(22) He, L.; Liu, Y.; Lin, M.; Mustapha, A.; Wang, Y. Detecting single *Bacillus* spores by surface enhanced Raman spectroscopy (SERS). *Sens. Instrum. Food Qual.* **2008**, in press.

(23) Alexander, T.; Le, D. Characterization of a commercialized SERS-active substrate and its application to the identification of intact *Bacillus* endospores. *Appl. Opt.* **2007**, *46*, 3878–3890.

(24) Le Ru, E. C.; Blackie, E.; Meyer, M.; Etchegoin, P. G. Surface enhanced Raman scattering enhancement factors: A comprehensive study. *J. Phys. Chem. C* **2007**, *111*, 13794–13803.

Received for review June 27, 2008. Revised manuscript received September 3, 2008. Accepted September 5, 2008.

JF801969V